Lung (2018) 196:633–642
https://doi.org/10.1007/s00408-018-0156-0

LUNG CANCER

Advances in Imaging and Automated Quantification of Malignant Pulmonary Diseases: A State-of-the-Art Review

Bruno Hochhegger[1,2] · Matheus Zanon[3] · Stephan Altmayer[3] · Gabriel S. Pacini[3] · Fernanda Balbinot[3] · Martina Z. Francisco[4] · Ruhana Dalla Costa[4] · Guilherme Watte[2,3] · Marcel Koenigkam Santos[5] · Marcelo C. Barros[4] · Diana Penha[6] · Klaus Irion[7] · Edson Marchiori[8]

Received: 31 May 2018 / Accepted: 28 August 2018 / Published online: 9 October 2018

Abstract

Quantitative imaging in lung cancer is a rapidly evolving modality in radiology that is changing clinical practice from a qualitative analysis of imaging features to a more dynamic, spatial, and phenotypical characterization of suspected lesions. Some quantitative parameters, such as the use of 18F-FDG PET/CT-derived standard uptake values (SUV), have already been incorporated into current practice as it provides important information for diagnosis, staging, and treatment response of patients with lung cancer. A growing body of evidence is emerging to support the use of quantitative parameters from other modalities. CT-derived volumetric assessment, CT and MRI lung perfusion scans, and diffusion-weighted MRI are some of the examples. Software-assisted technologies are the future of quantitative analyses in order to decrease intra- and inter-observer variability. In the era of "big data", widespread incorporation of radiomics (extracting quantitative information from medical images by converting them into minable high-dimensional data) will allow medical imaging to surpass its current status quo and provide more accurate histological correlations and prognostic value in lung cancer. This is a comprehensive review of some of the quantitative image methods and computer-aided systems to the diagnosis and follow-up of patients with lung cancer.

Keywords Lung cancer · Computed tomography · Magnetic resonance imaging · Positron emission tomography

Abbreviations

18F-FDG PET/CT	Fluorine-18-fluorodeoxyglucose positron emission tomography/computed tomography
ADC	Apparent diffusion coefficient
CAD	Computer-aided diagnosis
CT	Computed tomography
DCE	Dynamic contrast-enhanced
DTP	Dual time point imaging technique
DWI	Diffusion-weighted imaging
LSR	Lesion-to-spinal cord ratio
MRI	Magnetic resonance imaging
MRI-SI	Magnetic resonance imaging signal intensity
MVD	Microvessel density
NSCLC	Non-small cell lung cancer
RECIST	Response evaluation criteria in solid tumors
ROI	Regions of interest
SI	Signal intensity
SUV	Standardized uptake value
VDT	Volume doubling time

Introduction

Lung cancer represents 13% of total cancer incidence and 20% of cancer-related mortality worldwide [1]. During the last three decades, lung cancer prognosis has improved mainly due to efforts on early diagnosis and staging to target the growing number of available therapeutic options [2]. However, the overall prognosis remains poor with a 5-year survival rate of 15.6% [3].

Quantitative imaging modalities are promising methods to improve lung cancer identification and follow-up, as they use more accurate parameters than subjective analysis for assessment and prediction of treatment response, optimizing

✉ Bruno Hochhegger
brunoho@ufcspa.edu.br

Extended author information available on the last page of the article

care for individual patient [4]. Lung nodule measurement on computed tomography (CT) is an important quantitative marker to predict likelihood of malignancy and also progression of disease [5]. Fluorine-18-fluorodeoxyglucose positron emission tomography/computed tomography (18F-FDG PET/CT) provides information on the tumor's morphology, extension and glucose metabolism, outperforming CT or PET alone for lung cancer staging [6].

Advances in thoracic magnetic resonance imaging (MRI) have led to significant reduction in acquisition time and artifacts from respiratory and cardiac motion [7]. Recent MRI diffusion-weighted imaging (DWI) studies have reported accuracy comparable to PET/CT for evaluation of solid pulmonary lesions [8]. Lung perfusion imaging, such as dynamic enhanced CT and MRI, has also become a promising imaging technique to monitor lung malignancies by quantifying tumor blood flow and volume [9]. Software-assisted devices have also been more used to automate quantitative analyses and reduce intra- and inter-reader variability.

Considering all the recent advances in pulmonary imaging, our purpose was to review the modalities of quantitative lung cancer imaging and summarize some of the more promising computer-aided softwares to the diagnosis and follow-up of patients with lung cancer.

CT Nodule Measurement

Measurements of diameter or volume of pulmonary nodules provide important information for staging of malignancies and tumor growth during follow-up. When CT screening for lung cancer was first proposed, every indeterminate non-calcified nodule was followed with serial CT for a minimum of 2 years [10]. As this policy was not proved to be beneficial or cost-effective, the Fleischner Society proposed in 2005 a consensus for the assessment of incidental lung nodules based on nodule's size, growth rate, and risk factors for malignancy [11]. Solid nodules of up to 6 mm usually do not require routine follow-up. However, for high-risk patients, a 12-month follow-up examination is recommended. Nodules sized between 6 and 8 mm require one or two follow-up examinations over a period of 2 years. For nodules larger than 8 mm, management includes follow-up CT, PET/CT or tissue sampling at 3 months. In case of multiple nodules, the most suspicious nodule should be used as a reference for clinical management [11]. In the case of solitary sub-solid nodules, while no follow-up is recommended for those < 6 mm, further monitoring is advised for either part-solid or ground-glass nodules ≥ 6 mm depending on its characteristics [11].

Regarding therapy response evaluation in solid tumors, the response evaluation criteria in solid tumors (RECIST) is currently widely accepted. According to RECIST 1.1 [12], five is the maximum number of lesions required to assess tumor burden for response determination (and two per organ). To be considered a target lesion, a tumor must be of at least 10 mm in its longest diameter, while a lymph node is considered pathologically enlarged when is ≥ 15 mm in its short axis. Response to treatment may be considered: (a) complete, if all target lesions and all nodes with shortest axis < 10 mm disappeared; (b) partial, if there was at least 30% decrease in overall sum of target lesions (the sum of the longest diameters for non-nodal lesions and the shortest axis for lymph nodes) taking the baseline sum as reference; or (c) stable, if there was neither response or progression. Disease progression is defined as a 20% increase or a 5 mm absolute increase in the target lesions. The appearance of new malignant lesions not attributable to differences in scanning technique or change in imaging modality also denotes disease progression.

Some studies have analyzed whether it was appropriate to move from a linear to a volumetric anatomical assessment of tumor size [13–16]. Volumetric measurements are based on segmentation of nodules on thin-section CT data sets and an algorithm that translates the segmented voxels into nodule volume. Dicken et al. [16] compared the variability of a computer-aided volumetric assessment of lung lesions to manual measurements of in-plane lesion diameters performed according to RECIST. The volumetric assessments resulted in a markedly reduced variability of parameters describing size and change. The authors also showed that manual linear measurement requires a change of 2–3 mm to reliably detect a change on a typical lung lesion, whereas volumetric assessment is capable of detecting changes of about 1 pixel (~0.8 mm). For example, a nodule that has increased in diameter from 7 to 9 mm (2 mm or $> 25\%$ diameter increase in diameter) has approximately doubled its volume [17]. The "volume doubling time" (VDT) is currently accepted as the parameter to define a significant volume increased by means of volumetric analysis. A VDT of < 400 days yields a positive result for progression of disease according to the NELSON Trial [18].

Precision and accuracy of volume measurements depend on several factors, especially the software package used. Two authors have [19–21] showed substantial differences in segmentation performance among available software packages in a dataset of nodules with a variety in size, morphology, and contact to pulmonary structures. All software packages showed similar inter-examination variability but there were significant differences in absolute nodule volumes. Thus, despite the potential benefits of increased sensitivity and more robust detection of significant volume increase with small diameters changes, the lack of extensively validated software for volumetric nodule measurement still makes the linear measurement the current standard of practice [11].

Figure 1 presents a case of a spiculated pulmonary nodule follow-using the volumetric visual assessment.

18F-FDG PET/CT

18F-FDG PET/CT can provide both metabolic and anatomical information about the tumor. The quantitative parameter most commonly used to evaluate glucose metabolism in malignant cells is the standardized uptake value (SUV) corrected for body weight [11]. Although many different SUV cut-offs have been discussed, SUVmax (maximal SUV in the single hottest voxel) became the most popular parameter in oncology [22]. In this sense, SUVmax was shown to correlates well with disease prognosis in non-small cell lung cancer (NSCLC) [23, 24]. Also, a high SUV of the primary tumor determined by 18F-FDG PET prior to treatment is associated with a shorter time-to-progression, higher recurrence, and lower overall survival rates [25]. It has also been demonstrated that there is a low likelihood of a substantial response to therapy if there is no decrease in maximum SUV early after the initiation of anticancer treatment, representing a worse prognosis [26].

A relevant number of false-positive findings may occur with 18F-FDG PET/CT, especially infectious and inflammatory processes that may also present as an area of elevated glucose metabolism [27, 28]. The dual time point imaging technique (DTP) has been claimed to be a method to address this issue. The DTP protocol is based on reports that found that when SUV is measured sequentially, there is a correlation between 18F-FDG uptake and time. In malignant lesions, there is a continual increment of FDG uptake for several hours after its injection, whereas in inflammatory/infectious or normal tissues such increment in uptake is rare. Even though promising results were noted in some types of diseases, like lymphoma [29] and breast cancer [30], lung cancers did not seem to be significantly ameliorated by DTP imaging technique [31–33].

Besides the inherent risk of false-positive nodules with this modality, other disadvantages include high radiation dose, inconvenient pre-imaging protocols for patients, and low detection of small nodules with ground-glass attenuation (Fig. 2). Also, compared to CT or MR, PET/CT imaging is usually more costly to patients and scanners are not widely available [34].

Perfusion Computed Tomography

Perfusion is the transportation of blood to a tissue per unit of time [35]. Interpreting changes in lung perfusion parameters often translates into anomalous bloody supply patterns,

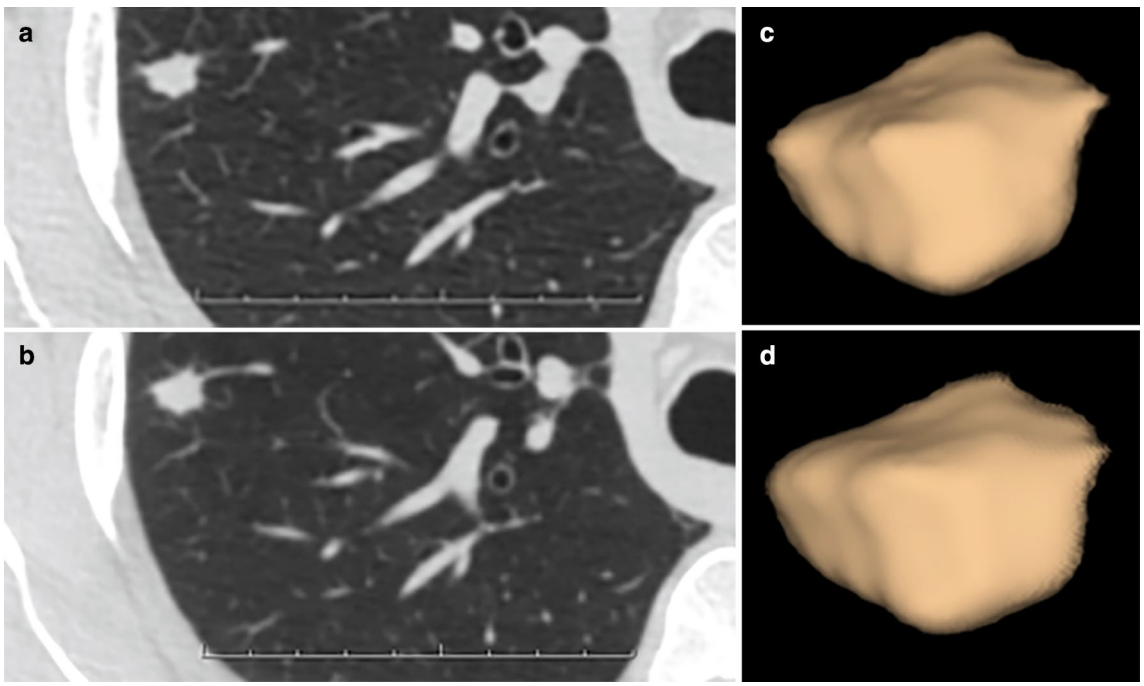

Fig. 1 Volumetric measurement of pulmonary nodule. Small, spiculate right upper lobe tumor on initial axial CT (**a**) showing minimal change in area by visual assessment on 4-month follow-up scan (**b**). (**c, d**) Three-dimensional CT scan obtained with volume rendering from 426 mm^3 on February 24, 2012 to 390 mm^3 on June 27, 2012. The volumetric assessment contributed to support a benign differential diagnosis in this case by detecting a 10% volume reduction that would likely pass unnoticed by linear or visual assessment. Outpatient follow-up revealed no progression of the lesion and the patient was managed conservatively

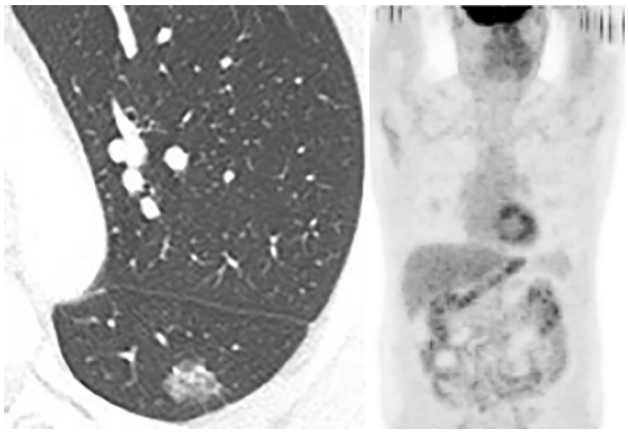

Fig. 2 CT scan with a ground-glass nodule in the left lung. PET/CT was performed and was negative. PET/CT is limited for these conditions and should not be used for small nodules with ground-glass attenuation

such as in tumor angiogenesis [36]. Higher perfusion in lung cancer has been found to be directly correlated with biomarkers of angiogenesis such as microvessel density (MVD) and hyperexpression of VEGF (vascular endothelial growth factor) [37, 38]. Given this correlation with VEGF expression, CT perfusion was shown to predict with imaging only responders to antiangiogenic tumor therapy [39]. Poorly perfused tumors, on the other hand, have been proved to be less responsive to chemotherapy (possibly because the chemotherapeutic agent is less efficiently delivered to the tumoral cells) and to radiotherapy (since they were more likely to be hypoxic) [40]. Besides, tumors with low perfusion rates have been reported to have an increased potential for lymph node metastases in advanced lung cancer [41].

There are two approaches to CT-derived lung perfusion imaging: the static peak enhancement imaging and the dynamic contrast-enhanced (DCE) imaging. The former consists of a single CT stop at a particular point of time—for instance, at the peak of normal lung parenchymal enhancement—so that changes in lung perfusion can be evidenced by differences in density of the lung tissue. The main advantage of this technique is that it is easily executed. However, disadvantages include inaccurate results in case of wrong timing and the fact that a single time point imaging cannot adequately represent physiologic differences in regional perfusion [42, 43]. On the other hand, DCE imaging gathers serial CT scans before and throughout the administration of iodinated contrast. Thus, temporal changes in contrast enhancement provide a time-signal intensity curve that allows a quantitative perfusion evaluation of the tissue. Different CT kinetic models are used to calculate perfusion parameters depending on the available software, but there is no consensus as to which is the optimal technique for assessment of tumor vascularity [43, 44].

Several authors have tried to use the principles of CT perfusion to aid in the differentiation of malignant and benign pulmonary nodules [45–47]. Parameters of perfusion per time in each nodule and blood volume have demonstrated accuracies of nearly 90% to rule out benign pulmonary lesions in the absence of perfusion and low blood volume [45]. Also, Ohno et al. using perfusion index was able to correctly identify as malignant three bronchoalveolar carcinomas misinterpreted as benign nodules by PET/CT [47]. Thus, although quantitative perfusion imaging by CT should be a promising modality in the characterization of indeterminate pulmonary nodules, the reliability and reproducibility of the functional results still represent an open issue. A high number of factors affecting the outcomes of CT perfusion examinations, such as imaging protocols, acquisition artifacts, and methods of data processing and analysis, are still to be validated [36].

Magnetic Resonance Imaging (MRI)

MRI Perfusion

The current approach to image lung perfusion by MRI is DCE imaging, which uses the same principles of DCE-CT: sequential imaging following the injection of a contrast agent, usually a gadolinium-based chelate. DCE-MRI was found to be suitable for discrimination of benign from malignant pulmonary nodules with sensitivity and specificity of 95% and 87%, respectively [48]. This method also proved to be valid to determine tumor's response to therapy [49]. A case in which MRI perfusion images were used to aid in the differential diagnosis of a solitary pulmonary nodule is shown in Fig. 3.

There are different DCE-MRI techniques described in medical literature, most of them are robust, simple to perform and can be applied in several clinical scenarios. The method is used for the evaluation of enhancement pattern and creation of signal intensity (SI)-time curves, which assures different derived quantitative parameters [50] (Fig. 4). In comparison to DCE-CT, DCE-MRI has the advantage of not requiring radiation exposure. However, while DCE-CT imaging is directly dependent on the concentration of contrast material in the blood, paramagnetic contrast material of DCE-MRI also depends on interactions among mobile water molecules in the interstitium and cytoplasm, creating a non-linear correlation between MRI-SI (magnetic resonance imaging signal intensity) and tissue contrast agent concentrations [51]. Although some models using high-relaxivity agents or non-linear corrections methods were proposed in an attempt to overcome this limitation [52], more advances in the area are required to the use of routine MRI perfusion imaging for solitary pulmonary nodules.

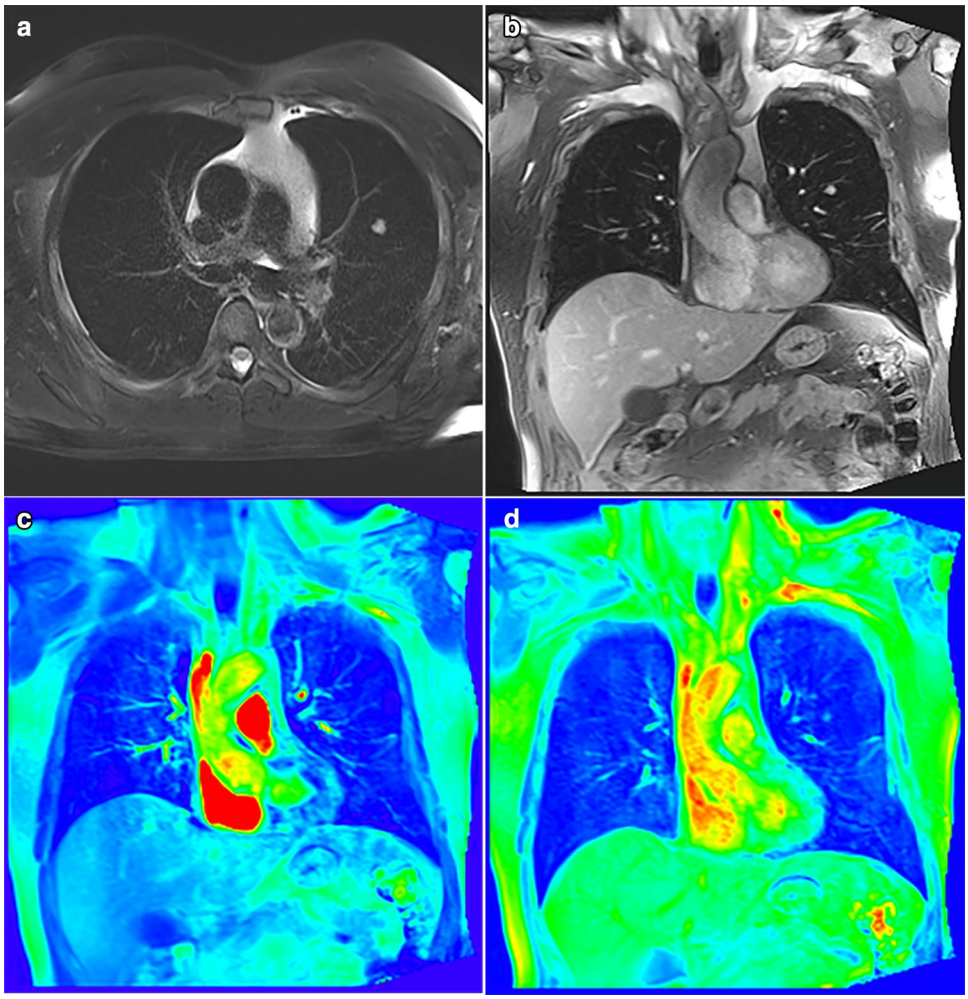

Fig. 3 MRI images (**a, b**) show a small solid nodule in the left upper lobe. In the perfusion images, a significant enhancement of the nodule is observed only in the pulmonary artery phase (**c**), but not in the subtraction image representing the bronchial artery phase (**d**)—supporting the diagnosis of a benign nodule. The patient decided through shared decision-making with his primary clinician to undergo a surgical lung biopsy to rule out malignancy, which revealed the diagnosis of cryptogenic organizing pneumonia

MRI Diffusion

Recent advances in MRI gradient technology have led to the introduction of DWI, which is entirely different from ordinary T1- and T2-weighted MRI images [53]. DWI-MRI has several advantages such as being a radiation-free method without the need for exogenous contrast medium, and it can provide quantitative and qualitative information about the integrity of cell membranes and tissue consistency [54]. Diffusion is the random, thermally induced movement of water molecules in biologic tissues, called Brownian motion. DWI is sensitive to molecular diffusion and allows for tissue characterization by probing tissue microstructural changes quantified as the apparent diffusion coefficient (ADC) [55].

In DWI-MRI, blood flow showing high diffusion and normal tissue with fat depression are undetectable [56]. Since malignant tumors have increased cellularity, larger nuclear/cytoplasmic ratio, and less extracellular space relative to normal tissue, the diffusion of water molecules in tumors is restricted, resulting in decreased ADC [7]. In fact, ADC was found to have an inverse correlation with PET/CT-derived SUVmax in NSCLC [57, 58]. DWI was shown to be equivalent to PET in distinguishing NSCLC from benign pulmonary nodules and also for detection of lymph node involvement [53, 58]. Pauls et al. [58] found that MRI with or without DWI agrees with PET/CT-derived N staging in most patients, with a tendency for an N understaging in 15% of patients.

DWI can differentiate malignant from benign pulmonary nodules in endemic areas of infectious diseases, where rates of false-positives in PET/CT are higher due to granulomatous lesions [59]. In this study, the lesion-to-spinal cord ratio (LSR) was also calculated to help differentiate malignant from benign lesions. The diagnostic capability of the ADC did not differ significantly from that of the LSR. However, LSR calculation is more useful and easily obtained than ADC in clinical routine practice. DWI can also be used for the differential diagnosis of solitary pulmonary hamartomas with inconclusive CT findings. Since almost 60% of pulmonary hamartomas contain fat, they were found to have no restriction in signal intensity on DWI sequence, but high signal intensity on T2-weighted sequences, suggesting that

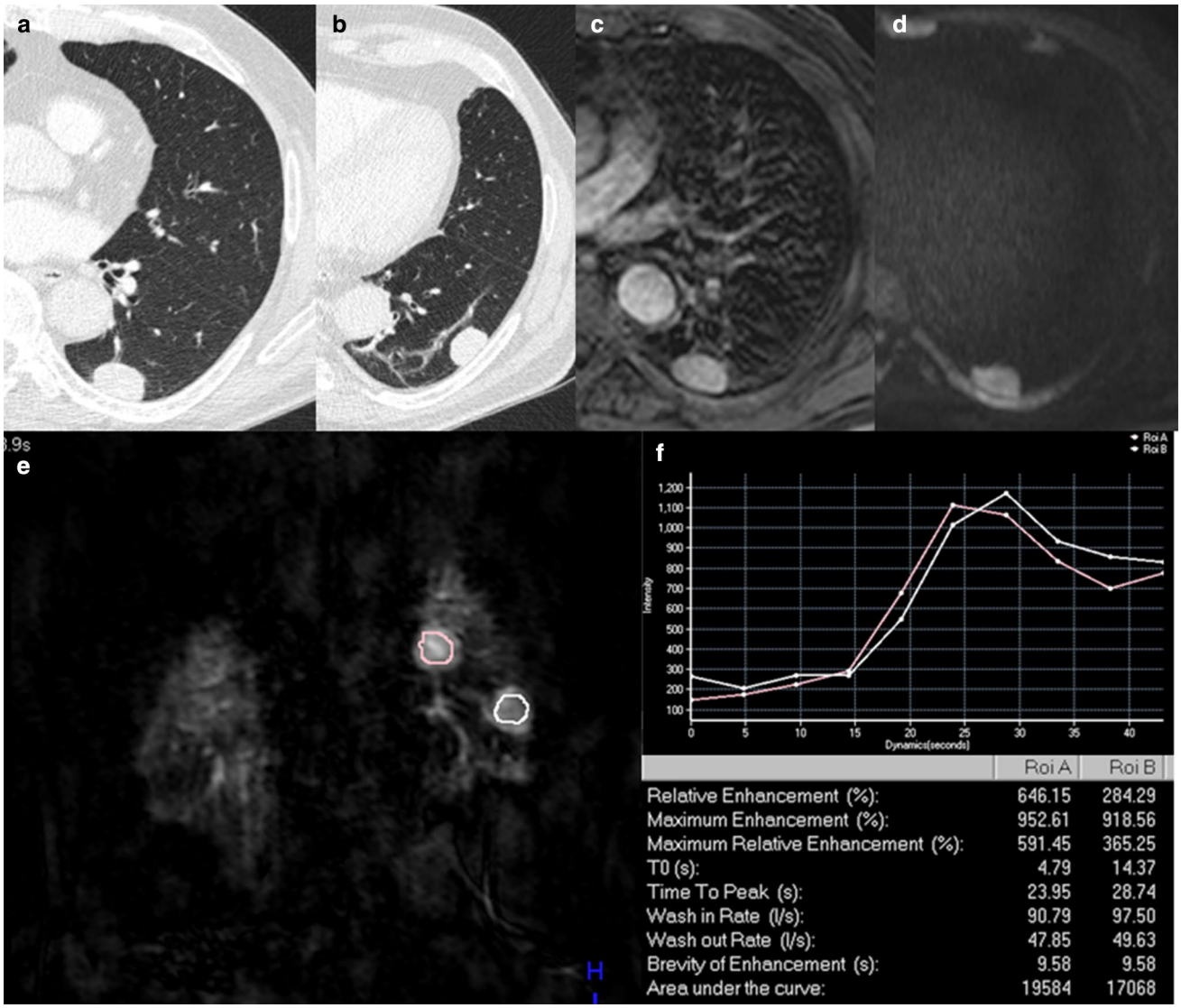

Fig. 4 Fifty two year-old male with history previously treated pulmonary tuberculosis presenting for evaluation of renal cell carcinoma. Staging CT images (**a, b**) demonstrating two peripheral round nodules on left lung. Lung MRI was performed to help characterize the lesions and showed significant post contrast enhancement (**c**) and restriction on DWI (**d**) (b-value of 1000). Perfusion analysis was also performed, showing an enhancement curve type A for both lesions, with fast and intense early SI increase followed by a fast and significant decrease (washout), as also demonstrated by the perfusion quantitative parameters (**e, f**). Biopsy proved both lesions to be metastases

chemical-shift MRI is accurate to distinguish hamartomas from other solitary pulmonary nodules [60]. Figure 5 represents a case in which MRI diffusion images were used to help in the differential diagnosis of solitary pulmonary nodule.

Radiomics of Lung Cancer (Artificial Intelligence)

Radiomics can be defined as the conversion of digital medical images into mineable high-dimensional data that can be quantitatively analyzed and correlated to different pathophysiological and clinical information [61]. Radiomics is a natural evolution of computer-aided diagnosis (CAD) systems. Whereas CAD systems traditionally provide single answers (for instance, the presence or not of a lesion), radiomics has been developed to provide prognostic information, aid in therapeutic decision, and correlate with clinical outcome. Thus, radiomics extracts and analyses quantitative information obtained with medical imaging that, combined with additional patients' characteristics, may provide more accurate diagnostic and prognostic value in clinical practice [62, 63].

In lung cancer, radiomics studies have been conducted using mainly CT and FDG-PET images. Radiomics texture

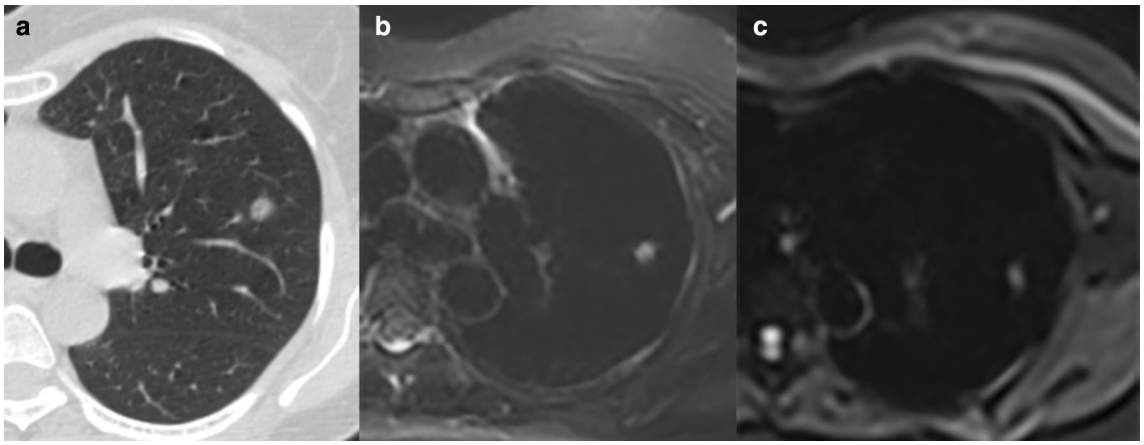

Fig. 5 Axial CT images, **a** demonstrating the presence of a sub-solid and ground-glass pulmonary nodules in the left upper lobe. **b, c** MRI images of the sub-solid nodule showed a T2 and diffusion-weighted sequences with hyperintense signal and restriction, respectively. Biopsy of the nodule confirms adenocarcinoma in situ, and the second an inflammatory lesion

analysis can be an independent marker of survival for patients with NSCLC as combining the radiomics signature with TNM staging showed a significant improvement in prognosis prediction [63, 64]. Radiomics features can reflect different biologic mechanisms, such as gene expression patterns or cell cycling pathways, and therefore capture distinct phenotypic differences between lung tumors [65, 66]. Radiomics principles have also been used to aid lung cancer histopathological subtype diagnosis ("virtual biopsy") and predict metastatic dissemination of NSCLC [67]. Figure 6 illustrates an example of radiomics evaluation.

Radiomics process begins with the acquisition of high-quality medical images. From acquired images, regions of interest (ROIs) that contain either the whole lesion or specific regions within the lesion are delineated. These ROIs are segmented and can also be rendered in three dimensions. Quantitative features and attributes are massively extracted from these ROIs to generate a report, which is placed in a database along with other patients and lesions'

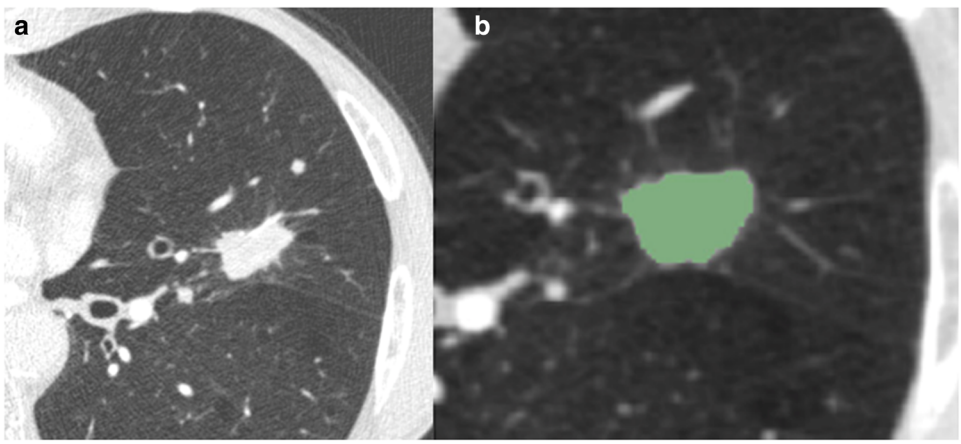

Fig. 6 Patient with a NSCLC adenocarcinoma, T1bN0M1b (bone). A spiculated nodule in lingula is identified on the lung window CT image (**a**). Nodule segmentation for the radiomic evaluation is highlighted in green color (**b**). Values of most significant image features for this lesion on a radiomic evaluation (relation to histology and metastasis) are also shown

data, combined to clinical, laboratory and genomic information. Then, these data are mined to develop diagnostic, predictive, or prognostic models for outcomes of interest [61]. Several qualitative and semi-quantitative features can be obtained based on lesions attenuation, such as heterogeneity, size, shape, margins, calcification, and cavitation. Other quantitative attributes based on lesions' shape, histogram, gray-level intensity, co-occurrence matrix texture, and more can be obtained [68].

The mining of radiomic data and correlation with biopsy-derived genomic information is known as radiogenomics [69]. There are only a few studies in chest imaging that tried to correlate CT radiomics with the expression of clinically relevant genetic mutations. Rizzo et al. were one of the groups that demonstrated that CT tumor features could predict EGFR mutation with a sensitivity and specificity of nearly 75% [70]. Association CT features and ALK mutation was also revealed by the same author and also Yamamoto et al. [70, 71]. Although the currently available results of radiogenomics are promising to noninvasively predict response to targeted therapy (e.g., tyrosine kinase inhibitors), the area still requires further validation in larger cohorts.

Overall, despite being a relatively recent topic, it is well established in literature that radiomics offers great potential in improving diagnosis of lung cancer, guiding therapy, and proving prognostic assessment. Radiomics may become part of clinical practice soon, as imaging is more often routinely used in medical practice worldwide and sharing of "big data" among different centers worldwide is increasing in research. It is also important to highlight that development of the radiomics signature is in accordance with the evolution and implementation of the personalized and precision medicine.

Conclusion

Advances in quantitative imaging techniques are becoming more widely available in clinical practice. Analysis and interpretation of quantitative imaging modalities can provide valuable information for diagnosis, staging, and treatment monitoring of patients with lung cancer.

Acknowledgements The authors thank Prof. Hans Ulrich Kauczor for his scientific contribution to improve this manuscript.

Compliance with Ethical Standards

Conflict of interest The authors declare that they have no conflict of interest.

References

1. McMahon PM, Kong CY, Johnson BE et al (2008) Estimating long-term effectiveness of lung cancer screening in the Mayo CT screening study. Radiology 248:278–287
2. Harders SW, Balyasnikowa S, Fischer BM (2014) Functional imaging in lung cancer. Clin Physiol Funct Imaging 34:340–355
3. Dela Cruz CS, Tanoue LT, Matthay RA (2011) Lung cancer: epidemiology, etiology, and prevention. Clin Chest Med 32:605–644
4. Yankeelov TE, Mankoff DA, Schwartz LH et al (2016) Quantitative imaging in cancer clinical trials. Clin Cancer Res: Off J Am Assoc Cancer Res 22(2):284–290
5. UyBico SJ, Wu CC, Suh RD et al (2010) Lung cancer staging essentials: the new TNM staging system and potential imaging pitfalls. Radiographics 30:1163–1181
6. Halpern BS, Schiepers C, Weber WA et al (2005) Presurgical staging of non-small cell lung cancer: positron emission tomography, integrated positron emission tomography/CT, and software image fusion. Chest 128:2289–2297
7. Henzler T, Schmid-Bindert G, Schoenberg SO et al (2010) Diffusion and perfusion MRI of the lung and mediastinum. Eur J Radiol 76:329–336
8. Matoba M, Tonami H, Kondou T et al (2007) Lung carcinoma: diffusion-weighted MR imaging—preliminary evaluation with apparent diffusion coefficient. Radiology 243:570–577
9. García-Figueiras R, Goh VJ, Padhani AR et al (2013) CT perfusion in oncologic imaging: a useful tool? Am J Roentgenol 200:8–19
10. Horeweg N, van Rosmalen J, Heuvelmans MA et al (2014) Lung cancer probability in patients with CT-detected pulmonary nodules: a prespecified analysis of data from the NELSON trial of low-dose CT screening. Lancet Oncol 15:1332–1341
11. MacMahon H, Naidich DP, Goo JM et al (2017) Guidelines for management of incidental pulmonary nodules detected on CT images: from the Fleischner Society 2017. Radiology 284(1):228–243
12. Eisenhauer EA, Therasse P, Bogaerts J et al (2009) New response evaluation criteria in solid tumours: revised RECIST guideline (version 1.1). Eur J Cancer 45:228–247
13. Galizia M, Töre H, Chalian H et al (2011) Evaluation of hepatocellular carcinoma size using two-dimensional and volumetric analysis. Acad Radiol 14:1555–1560
14. Marten K, Auer F, Schmidt S et al (2007) Automated CT volumetry of pulmonary metastases: the effect of a reduced growth threshold and target lesion number on the reliability of therapy response assessment using RECIST criteria. Eur Radiol 17:2561–2571
15. Vogel M, Schmücker S, Maksimovic O et al (2012) Reduction in growth threshold for pulmonary metastases: an opportunity for volumetry and its impact on treatment decisions. Br J Radiol 85:959–964
16. Dicken V, Bornemann L, Moltz JH et al (2015) Comparison of volumetric and linear serial CT assessments of lung metastases in renal cell carcinoma patients in a clinical phase IIB study. Acad Radiol 22:619–625
17. Bankier AA, MacMahon H, Goo JM et al (2017) Recommendations for measuring pulmonary nodules at CT: a statement from the Fleischner Society. Radiology 285:584–600
18. Yousaf-Khan U, van der Aalst C, de Jong PA et al (2017) Final screening round of the NELSON lung cancer screening trial: the effect of a 2.5-year screening interval. Thorax 72(1):48–56
19. de Hoop B, Gietema H, van Ginneken B et al (2009) A comparison of six software packages for evaluation of solid lung nodules using semiautomated volumetry: what is the minimum

increase in size to detect growth in repeated CT examinations. Eur Radiol 19:800–808
20. Zhao YR, van Ooijen PM, Dorrius MD et al (2014) Comparison of three software systems for semi-automatic volumetry of pulmonary nodules on baseline and follow-up CT examinations. Acta Radiol 55:691–698
21. Kuhnert G, Boellaard R, Sterzer S et al (2016) Impact of PET/CT image reconstruction methods and liver uptake normalization strategies on quantitative image analysis. Eur J Nucl Med Mol Imaging 43:249–258
22. Boellaard R, Delgado-Bolton R, Oyen WJG et al (2015) FDG PET and PET/CT: EANM procedure guidelines for tumour PET imaging: version 2.0. Eur J Nucl Med Mol Imaging 42:328–354
23. Markovina S, Duan F, Snyder BS et al (2015) Regional lymph node uptake of [(18)F]fluorodeoxyglucose after definitive chemoradiation therapy predicts local-regional failure of locally advanced non-small cell lung cancer: results of ACRIN 6668/RTOG 0235. Int J Radiat Oncol Biol Phys 93:597–605
24. Paesmans M, Garcia C, Wong CO et al (2015) Primary tumour standardised uptake value is prognostic in nonsmall cell lung cancer: a multivariate pooled analysis of individual data. Eur Respir J 46:1751–1761
25. Cerfolio RJ, Bryant AS, Ohja B et al (2005) The maximum standardized uptake values on positron emission tomography of a non-small cell lung cancer predict stage, recurrence, and survival. J Thorac Cardiovasc Surg 130:151–159
26. Nahmias C, Hanna WT, Wahl LM et al (2007) Time course of early response to chemotherapy in non-small cell lung cancer patients with 18F-FDG PET/CT. J Nucl Med 48:744–751
27. Gupta NC, Tamim WJ, Graeber GG et al (2001) Mediastinal lymph node sampling following positron emission tomography with fluorodeoxyglucose imaging in lung cancer staging. Chest 120:521–527
28. Roberts PF, Follette DM, von Haag D et al (2000) Factors associated with false-positive staging of lung cancer by positron emission tomography. Ann Thorac Surg 70:1154–1159
29. Nakayama M, Okizaki A, Ishitoya S et al (2013) Dual-time-point F-18 FDG PET/CT imaging for differentiating the lymph nodes between malignant lymphoma and benign lesions. Ann Nucl Med 27:163–169
30. Kumar R, Loving VA, Chauhan A et al (2005) Potential of dual-time-point imaging to improve breast cancer diagnosis with (18) F-FDG PET. J Nucl Med 46:1819–1824
31. Sathekge MM, Maes A, Pottel H et al (2010) Dual time-point FDG PET-CT for differentiating benign from malignant solitary pulmonary nodules in a TB endemic area. S Afr Med J 100:598–601
32. Kaneko K, Sadashima E, Irie K et al (2013) Assessment of FDG retention differences between the FDG-avid benign pulmonary lesion and primary lung cancer using dual-time-point FDG-PET imaging. Ann Nucl Med 27:392–399
33. Saleh Farghaly HR, Mohamed Sayed MH, Nasr HA et al (2015) Dual time point fluorodeoxyglucose positron emission tomography/computed tomography in differentiation between malignant and benign lesions in cancer patients. Does it always work? Indian J Nucl Med 30:314–319
34. Wong CS, Gong N, Chu YC et al (2012) Correlation of measurements from diffusion weighted MR imaging and FDG PET/CT in GIST patients: ADC versus SUV. Eur J Radiol 81:2122–2126
35. Usaro A, Ruokonen E, Takala J (1995) Estimation of splanchnic blood flow by the Fick principle in man and problems in the use of indocyanine green. Cardiovasc Res 30:106–112
36. Bevilacqua A, Barone D, Malavasi S et al (2014) Quantitative assessment of effects of motion compensation for liver and lung tumors in CT perfusion. Acad Radiol 21:1416–1426
37. Li Y, Yang ZG, Chen TW et al (2008) Peripheral lung carcinoma: correlation of angiogenesis and first-pass perfusion parameters of 64-detector row CT. Lung Cancer 61:44–53
38. Ma SH, Le HB, Jia BH et al (2008) Peripheral pulmonary nodules: relationship between multi-slice spiral CT perfusion imaging and tumor angiogenesis and VEGF expression. BMC Cancer 8:186
39. Ma S-H, Le H-B, Jia B et al (2008) Peripheral pulmonary nodules: relationship between multi-slice spiral CT perfusion imaging and tumor angiogenesis and VEGF expression. BMC Cancer 8:186
40. Wang J, Wu N, Cham MD et al (2009) Tumor response in patients with advanced non-small cell lung cancer: perfusion CT evaluation of chemotherapy and radiation therapy. AJR Am J Roentgenol 193:1090–1096
41. Huellner MW, Collen TD, Gut P et al (2014) Multiparametric PET/CT-perfusion does not add significant additional information for initial staging in lung cancer compared with standard PET/CT. EJNMMI Res 4:6
42. Mirsadraee S, van Beek EJR (2015) Functional imaging: computed tomography and MRI. Clin Chest Med 36:349–363
43. O'Connor JP, Tofts PS, Miles KA et al (2011) Dynamic contrast-enhanced imaging techniques: CT and MRI. Br J Radiol 84:S112–S120
44. Petralia G, Preda L, D'Andrea G et al (2010) CT perfusion in solid-body tumours. Part I: technical issues. Radiol Med 115:843–857
45. Li Y, Yang Z-G, Chen T-W, Yu J-Q, Sun J-Y, Chen H-J (2010) First-pass perfusion imaging of solitary pulmonary nodules with 64-detector row CT: comparison of perfusion parameters of malignant and benign lesions. Br J Radiol 83(993):785–790
46. Yuan X, Zhang J, Quan C et al (2013) Differentiation of malignant and benign pulmonary nodules with first-pass dual-input perfusion CT. Eur Radiol 23(9):2469–2474
47. Ohno Y, Koyama H, Matsumoto K et al (2011) Differentiation of malignant and benign pulmonary nodules with quantitative first-pass 320-detector row perfusion CT versus FDG PET/CT. Radiology 258(2):599–609
48. Jiang B, Liu H, Zhou D (2016) Diagnostic and clinical utility of dynamic contrast-enhanced MR imaging in indeterminate pulmonary nodules: a metaanalysis. Clin Imaging 40:1219–1225
49. Cheng JC, Yuan A, Chen JH et al (2013) Early detection of Lewis lung carcinoma tumor control by irradiation using diffusion-weighted and dynamic contrast-enhanced MRI. PLoS ONE 8:e62762
50. Koenigkam-Santos M, Optazaite E, Sommer G et al (2015) Contrast-enhanced magnetic resonance imaging of pulmonary lesions: description of a technique aiming clinical practice. Eur J Radiol 84:185–192
51. Schaefer JF, Vollmar J, Schick F et al (2004) Solitary pulmonary nodules: dynamic contrast-enhanced MR imaging–perfusion differences in malignant and benign lesions. Radiology 232:544–553
52. Bell LC, Wang K, Munoz Del Rio A et al (2015) Comparison of models and contrast agents for improved signal and signal linearity in dynamic contrast-enhanced pulmonary magnetic resonance imaging. Invest Radiol 50:174–178
53. Ohba Y, Nomori H, Mori T et al (2009) Is diffusion-weighted magnetic resonance imaging superior to positron emission tomography with fludeoxyglucose F 18 in imaging non-small cell lung cancer? J Thorac Cardiovasc Surg 138:439–445
54. Li B, Li Q, Chen C et al (2014) A systematic review and meta-analysis of the accuracy of diffusion-weighted MRI in the detection of malignant pulmonary nodules and masses. Acad Radiol 21:21–29
55. Wu LM, Xu JR, Hua J et al (2013) Can diffusion-weighted imaging be used as a reliable sequence in the detection of malignant pulmonary nodules and masses? Magn Reson Imaging 31:235–246

56. Usuda K, Zhao XT, Sagawa M et al (2011) Diffusion-weighted imaging is superior to positron emission tomography in the detection and nodal assessment of lung cancers. Ann Thorac Surg 91:1689–1695
57. Regier M, Derlin T, Schwarz D et al (2012) Diffusion weighted MRI and 18F-FDG PET/CT in non-small cell lung cancer (NSCLC): does the apparent diffusion coefficient (ADC) correlate with tracer uptake (SUV)? Eur J Radiol 81:2913–2918
58. Pauls S, Schmidt SA, Juchems MS et al (2012) Diffusion-weighted MR imaging in comparison to integrated [^{18}F]-FDG PET/CT for N-staging in patients with lung cancer. Eur J Radiol 81:178–182
59. Henz-Concatto N, Watte G, Marchiori E et al (2016) Magnetic resonance imaging of pulmonary nodules: accuracy in a granulomatous disease-endemic region. Eur Radiol 26:2915–2920
60. Hochhegger B, Marchiori E, dos Reis DQ et al (2012) Chemical-shift MRI of pulmonary hamartomas: initial experience using a modified technique to assess nodule fat. AJR Am J Roentgenol 199:W331–W334
61. Gillies R, Kinahan P, Hricak H (2016) Radiomics: images are more than pictures, they are data. Radiology 278:563–577
62. Doi K (2007) Computer-aided diagnosis in medical imaging: historical review, current status and future potential. Comput Med Imaging Graph 31:198–211
63. Aerts HJ, Velazquez ER, Leijenaar RT et al (2014) Decoding tumour phenotype by noninvasive imaging using a quantitative radiomics approach. Nat Commun 5:400665
64. Ganeshan B, Panayiotou E, Burnand K et al (2012) Tumour heterogeneity in non-small cell lung carcinoma assessed by CT texture analysis: a potential marker of survival. Eur Radiol 22:796–802
65. Fried DV, Tucker SL, Zhou S et al (2014) Prognostic value and reproducibility of pretreatment CT texture features in stage III non-small cell lung cancer. Int J Radiat Oncol Biol Phys 90:834–842
66. Yoon HJ, Sohn I, Cho JH et al (2015) Decoding tumor phenotypes for ALK, ROS1, and RET fusions in lung adenocarcinoma using a radiomics approach. Medicine (Baltimore) 94:e1753
67. Ferreira-Junior JR, Koenigkam-Santos M, Cipriano FEG et al (2018) Radiomics-based features for pattern recognition of lung cancer histopathology and metastases. Comput Methods Programs Biomed 159:23–30
68. Yang J, Zhang L, Fave X (2016) Uncertainty analysis of quantitative imaging features extracted from contrast-enhanced CT in lung tumors. Comput Med Imaging Graph 48:1–8
69. Guo Z, Shu Y, Zhou H et al (2015) Radiogenomics helps to achieve personalized therapy by evaluating patient responses to radiation treatment. Carcinogenesis 36:307–317
70. Rizzo S, Petrella F, Buscarino V et al (2016) CT radiogenomic characterization of EGFR, K-RAS, and ALK mutations in non-small cell lung cancer. Eur Radiol 26:32–42
71. Yamamoto S, Korn RL, Oklu R et al (2014) ALK molecular phenotype in non-small cell lung cancer: CT radiogenomic characterization. Radiology 272:568–576

Affiliations

Bruno Hochhegger[1,2] · Matheus Zanon[3] · Stephan Altmayer[3] · Gabriel S. Pacini[3] · Fernanda Balbinot[3] · Martina Z. Francisco[4] · Ruhana Dalla Costa[4] · Guilherme Watte[2,3] · Marcel Koenigkam Santos[5] · Marcelo C. Barros[4] · Diana Penha[6] · Klaus Irion[7] · Edson Marchiori[8]

Matheus Zanon
mhgzanon@hotmail.com

Stephan Altmayer
stephanaltmayer@gmail.com

Gabriel S. Pacini
gabrielsartorip@gmail.com

Fernanda Balbinot
balbinotf@gmail.com

Martina Z. Francisco
martinazfrancisco@gmail.com

Ruhana Dalla Costa
ruhanadalla@gmail.com

Guilherme Watte
g.watte@gmail.com

Marcel Koenigkam Santos
marcelk46@fmrp.usp.br

Marcelo C. Barros
macardosob@hotmail.com

Diana Penha
dianapenha@gmail.com

Klaus Irion
klaus.irion@cmft.nhs.uk

Edson Marchiori
edmarchiori@gmail.com

1 LABIMED – Medical Imaging Research Lab, Department of Radiology, Pavilhão, Pereira Filho Hospital, Irmandade Santa Casa de Misericórdia de Porto Alegre, Av. Independência, 75, Porto Alegre 90020-160, Brazil

2 Department of Imaging, Pontifical Catholic University of Rio Grande do Sul, Av. Ipiranga, 6681 - Partenon, Porto Alegre, RS 90619-900, Brazil

3 Medical Imaging Research Laboratory, Federal University of Health Sciences of Porto Alegre, R. Sarmento Leite, 245, Porto Alegre, Rio Grande Do Sul 90050-170, Brazil

4 Department of Radiology, Irmandade da Santa Casa de Misericordia de Porto Alegre, Av. Independência, 75, Porto Alegre 90035-072, Brazil

5 Ribeirao Preto Medical School, Av. Bandeirantes, 3900, Monte Alegre, Ribeirão Preto, São Paulo 14049-900, Brazil

6 Radiology, Liverpool Heart and Chest Hospital, Thomas Dr, Liverpool L14 3PE, UK

7 Central Manchester University Hospitals NHS Foundation Trust, Manchester Royal Infirmary, Oxford Road, Manchester M13 9WL, UK

8 Federal University of Rio de Janeiro, Av. Carlos Chagas Filho, 373, Rio De Janeiro 21941-902, Brazil